

# On Neutral Unsaturated Ouroboric Borylenes

Kelling J. Donald,\* Ulrick R. Gaillard,<sup>†</sup> and Noah Walker<sup>‡</sup>



Cite This: *J. Phys. Chem. A* 2022, 126, 5173–5185



Read Online

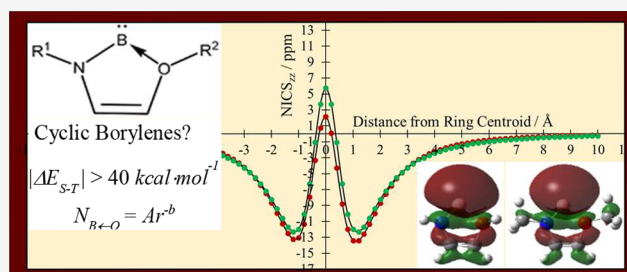
ACCESS |

Metrics & More

Article Recommendations

Supporting Information

**ABSTRACT:** The search is on for stable isolated borylenes. Potential roles in modern synthetic chemistry for boron analogues of carbenes continue to motivate interest in locating them. Using density functional and ab initio methods, we posit and examine the thermochemistry, and chemical bonding, including aromaticity, of several classes of 5- and 6-membered borylenic rings. In these systems, cyclization relies on dative bonding (ouroboric coordination) and  $\pi$  donation to a monovalent boron center from an adjacent O center. Certain neutral five-membered rings (heterocyclic cyclopentadienyl analogues) in particular are found to exhibit exceptionally strong preferences for the singlet multiplicity, each with singlet–triplet (S–T) gaps in excess of 40 kcal·mol<sup>-1</sup>. The singlet five-membered rings with the largest S–T gaps and some of the six-membered rings show evidence of weak aromaticity. Relationships of the form  $N = A \cdot r^{-b}$ , in line with Gordy's and other functions linking bond order,  $N$ , and covalent bond length, are identified for dative B←O contacts,  $r$ , reinforced in rings by  $\pi$ -delocalization.



## INTRODUCTION

What are the necessary conditions for borylene stability? The implicit analogy between carbenes,  $:\text{CRR}'$ , and neutral borylenes as well as boryl anions (systems such as  $:\text{B}-\text{R}$  and  $:\text{BRR}'$ , respectively)<sup>1–3</sup> motivates the ongoing search for stable borylenes. This is not just because of the evident electronic analogy between carbenes and borylenes, but current difficulties in preparing (not to mention bottling) neutral borylenes reminds us too of the initial difficulties in finding stable carbenes.<sup>4–6</sup> That the barriers to the latter were eventually overcome<sup>7</sup> offers hope to some that thermodynamic stability and kinetic persistence may be achievable for borylenes as well. But boron is not carbon, and the path to stable borylenes is evidently not straightforward.

Several simple free borylenes, such as  $:\text{B}-\text{R}$  for  $\text{R} = \text{H}$ ,<sup>8,9</sup>  $\text{F}$ ,<sup>10,11</sup>  $\text{Cl}$ ,<sup>12</sup>  $\text{Br}$ ,<sup>13</sup>  $\text{I}$ ,<sup>14</sup> and  $\text{Ph}$ ,<sup>15</sup> have been examined extensively, some having been identified decades ago.<sup>16–22</sup> “Note on the Spectrum of Boron Fluoride” was published in 1935,<sup>23</sup> for example, and referenced two slightly earlier and less successful (ultraviolet) spectroscopic studies of  $\text{BF}$ .<sup>24,25</sup> Those investigations were motivated in part by the already extensive data available on the isovalent  $\text{CO}$  and  $\text{N}_2$  molecules, but unlike  $\text{N}_2$ ,  $\text{BF}$  and other simple  $:\text{B}-\text{R}$  molecules tend to be unstable and have been detected and probed primarily in the gas phase or in inert matrices.<sup>8–15,23–27</sup>

Borylenes may be trapped, however, as ligands coordinated in some way to metal,  $\text{M}$ , and other atomic centers in  $\text{M}=\text{B}-\text{R}$ <sup>28–30</sup> or  $\text{M} \leftarrow \text{B}-\text{R}$ <sup>31,32</sup> type complexes, and there has been impressive progress in those general directions.<sup>9,33,34</sup> A related and equally intriguing class of borylene complexes are those in which a  $\text{BR}$  fragment is stabilized by donation into one or both

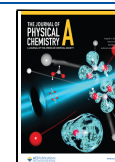
of the empty orbitals on the B center.<sup>29,35–38</sup> The growing interest in the fundamental properties of borylenes has been followed closely by efforts to identify (both experimentally and computationally) practical applications of neutral borylenes (and boryl anions<sup>2</sup>) in chemistry. Areas of progress along those lines include the activation of chemical bonds (including C–H, and C–C bonds)<sup>1,39–43</sup> and boron-mediated  $\text{CO}$  activation and  $\text{N}_2$  fixation (for example, see refs 38 and 44–51 and references therein). The compounds that have found success in such experimental applications beyond the gas phase, however, are typically terminal metal complexes with coordinated borylenes ( $\text{M}=\text{B}-\text{R}$ ), as distinguished from free borylenes ( $:\text{B}-\text{R}$ ),<sup>44</sup> due to the high and rather indiscriminate reactivity of the latter species.

Yet, the dream is alive. Despite earlier disputes about mechanisms invoking methylborylene (obtained using  $\text{CH}_3\text{BBr}_2$  with  $\text{C}_8\text{K}$  or  $\text{Na/K}$ ) as an intermediate in addition and C–H insertion reactions,<sup>19</sup> reliable evidence is available for borylenes as reactive intermediates.<sup>1,21,39,40,52,53</sup> And the search for more stable free borylenes is yielding already some interesting computational insights: Lu et al. investigated the electronic structures of several model  $:\text{B}-\text{R}$  species stabilized by intra- and intermolecular coordination to N lone pairs or carbenes,<sup>54</sup> and Bharadwaz and Phukan identified tricyclic N-

Received: June 20, 2022

Revised: July 15, 2022

Published: July 29, 2022



heterocyclic borylenes with singlet–triplet energy (S–T) gaps of up to 30 kcal·mol<sup>-1</sup>.<sup>55</sup> The latter systems featured a central six-membered (C<sub>3</sub>NBN) ring flanked (along the C–N bonds) by two fused four-membered ylidic rings, with a covalent N–B bond and a  $\sigma$  dative :B←N bond in the six-membered central ring.

We have been interested more recently in spontaneous ouroboric cyclization by dative bonding, where one end of a chain latches on to the other without breaking  $\sigma$ -bonds.<sup>56,57</sup> There are established experimental instances of B←O  $\sigma$ -bonding as a driver for self-healing in polymers (see refs 58 and 59, for example) and ring closure by boron(III)←oxygen dative bonding has been demonstrated repeatedly as well.<sup>60,61</sup> We propose in this contribution a series of neutral singlet monocyclic borylenes based on an ouroboric B(I)←O bonding motif. Large singlet–triplet gaps, several in excess of those mentioned previously for N-heterocyclic borylenes, are achieved by  $\sigma$  donation from an oxygen center to a boron(I) center supported by some  $\pi$ -delocalization in five- and six-membered rings. A (4*n* + 2) Hückel number of electrons confers in some cases a certain degree of aromaticity on the minimum energy borylene rings.

## COMPUTATIONAL METHODS

We considered at the outset several unprecedented bonding motifs for neutral five- and six-membered borylene type rings. To identify the candidates that were most viable electronically as singlet cyclic borylenes, structural optimizations and harmonic vibrational frequency analyses were completed using the B3LYP<sup>62</sup> method (with the ultrafine grid as defined in the Gaussian 09 suite of programs<sup>63</sup>) paired with the correlation-consistent triple- $\zeta$  (cc-pVTZ)<sup>64</sup> basis sets. That level of theory allowed us to make contact with earlier calculations on borylenes,<sup>54</sup> but the systems that persisted as singlet cyclic borylenes after that optimization were then reoptimized at the B3LYP-D3BJ,<sup>62,65,66</sup> M06,<sup>67</sup> M06-2X,<sup>67</sup>  $\omega$ B97XD,<sup>68</sup> and MP2(full)<sup>69,70</sup> levels of theory along with the same basis sets. For the latter persistent ring systems, all subsequent analyses have been carried out at the  $\omega$ B97XD level, accounting more reliably (relative to the B3LYP method) for dispersion.

Structural optimizations and frequency analyses have been carried out at the CCSD(T)<sup>71</sup> level as well for certain small model borylene, carbene, and analogous reference systems. Those calculations (and experimental data in some cases) provide a basis for assessing the reliability, for instance, of singlet–triplet energy gap values obtained herein using some of the other less computationally intensive methods. The planarity, stability, and  $\pi$  electron counts in several of the optimized borylenic ring systems examined implies  $\pi$  delocalization in those species. Aromatic stabilization energies (ASE)<sup>72</sup> and nucleus independent chemical shift (NICS)<sup>73</sup> calculations have been performed to evaluate the aromatic character of the rings. We report, specifically, scans of the *zz*-tensor components of the NICS (NICS<sub>zz</sub>), which are considered to be reliable indicators of aromaticity for small ring systems.<sup>74</sup> NICS scans that extend from the ring centroid to 10.0 Å in 0.2 Å increments above and below the best-fit plane for the ring of atoms have been generated. It was necessary to locate the best-fit plane and to carry out this assessment in both directions since, in some cases, the rings were not completely flat or branching substituents reduced symmetry. Representations of molecular structures and

molecular orbital pictures in this work were obtained using the GaussView<sup>75</sup> and Chemcraft<sup>76</sup> programs. Unless stated otherwise, as in the case of any transition state structure, all structural data are for minima, confirmed by vibrational frequency analyses to have no imaginary frequency at the relevant level of theory.

## RESULTS AND DISCUSSION

**Borylene Considerations.** We have examined a set of 72 cyclic borylenic systems based on eight proposed five- and six-membered heterocyclic ring frameworks. The systems that we considered, as summarized in Figure 1, have at least one valid

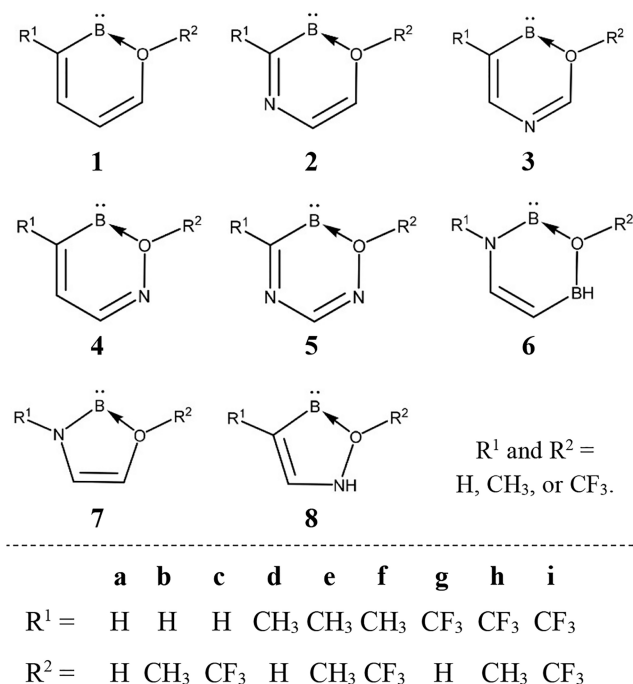


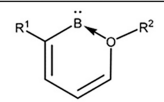
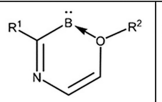
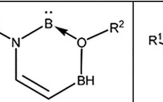
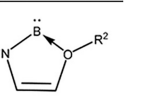
**Figure 1.** Seventy-two candidate cyclic structures considered in this work.

cyclic aromatic resonance form in which the ring is closed by a dative (coordinate covalent)  $\sigma$  bond between a monovalent boron and an oxygen center, and that B←O  $\sigma$ -bond is reinforced potentially by  $\pi$ -delocalization around the ring.

In the ouroboric electronic arrangements in Figure 1, all four of the valence orbitals of the nominally *sp*<sup>2</sup> hybridized boron center are potentially involved in bonding (with a covalent B–N  $\sigma$  bond, a dative B←O  $\sigma$  bond, a *p* orbital engaged in some degree of  $\pi$  delocalization, and a lone pair). If such a resonance form is dominant, the localization of the lone pair is expected to be a prominent feature of each system.

As drawn in Figure 1, the rings are able formally to satisfy Hückel's rule by engaging a pair of electrons on O and the two double bonds in 1–5 (Figure 1) or a pair of electrons each from the O and N centers in 6–8 along with the one C=C double bond in those structures. Yet, there are any number of other potentially competitive resonance forms and nonplanar conformations for many of the classes of structures shown in Figure 1, so it was understood at the outset that the proposed rings may be unstable relative to alternative bonding arrangements.

**Table 1. Twenty-Eight Singlet Cases Where Cyclic Borylene-like (B3LYP) Minimum Energy Structures Were Located (Indicated by a Tick)<sup>a</sup>**

						
	R <sup>1</sup>	R <sup>2</sup>	<b>1</b>	<b>2</b>	<b>6</b>	<b>7</b>
<b>a.</b>	H	H	✓	✓	✓	✓ <sup>c</sup>
<b>b.</b>	H	CH <sub>3</sub>	✓	✓ Distorted <sup>a</sup>	✓	✓
<b>c.</b>	H	CF <sub>3</sub>	*	Chain <sup>b</sup>	*	*
<b>d.</b>	CH <sub>3</sub>	H	✓	✓	✓	✓ <sup>c</sup>
<b>e.</b>	CH <sub>3</sub>	CH <sub>3</sub>	✓	✓	✓	✓
<b>f.</b>	CH <sub>3</sub>	CF <sub>3</sub>	*	Chain <sup>b</sup>	*	*. <sup>c</sup>
<b>g.</b>	CF <sub>3</sub>	H	✓	✓ Distorted <sup>a</sup>	✓	✓ <sup>c</sup>
<b>h.</b>	CF <sub>3</sub>	CH <sub>3</sub>	✓ Distorted <sup>a</sup>	✓ Distorted <sup>a</sup>	✓	✓
<b>i.</b>	CF <sub>3</sub>	CF <sub>3</sub>	*	✓ Distorted <sup>a</sup>	Chain <sup>b</sup>	*. <sup>c</sup>

<sup>a</sup>Key: (\*) The ring opens up with an O→B interatomic separation that is larger than 2.5 Å, but the structure remains planar, indicative possibly of a weak van der Waals type interaction between the O and B centers in the chain. Compare to the O→B contacts in the other planar structures which are less than 1.75 Å at the B3LYP level. (a) Optimized structure is a distorted ring. (b) The ring opens to form a chain. (c) The O-R<sup>2</sup> bond is out of the plane of the ring. (d) Of the nine 3a–3i systems, only 3b, 3d, and 3e optimized to give a closed planar (3d) or distorted (3b, and 3e) ring as a minimum energy structure. No cyclic borylene-like structure was obtained for systems 4, 5, or 8.

**Ring Stability.** To assess, therefore, the stability of all seventy-two species (1–8, with R<sup>1</sup>/R<sup>2</sup> substituents a–i in Figure 1), we carried out full (singlet) geometry optimizations and frequency analyses at the B3LYP level of theory using conformations shown in Figure 1 as the initial geometries. For those starting structures, the rings were planar and the B←O contacts were between 1.60 and 2.00 Å, which is above the sum of the covalent radii of B and O (0.85 Å + 0.63 Å = 1.48 Å)<sup>77</sup> but well below the sum of the van der Waals radii of B and O (2.08 Å + 1.40 Å = 3.48 Å).<sup>78</sup> The B3LYP method neglects dispersion interactions, but we are primarily interested at the start of this assessment in dative bonds with substantial covalent contributions, and in that regard the use of the B3LYP method at this point offers an advantage for screening. We have found no previous report on intramolecular borylenes with B←O ouroboric contacts, but the use of the B3LYP method at this stage makes contact as well with previous investigations on potential borylenic systems.<sup>54</sup>

The outcomes of our initial optimizations were quite instructive. Only the bonding motifs labeled 1, 2, 3, 6, and 7 in Figure 1 gave any minimum energy structure that retained a cyclic (be it planar or puckered) arrangement for any of their nine substituent combinations (a–i). System 4 generally recyclized by breaking the O–N bond and establishing a B–N bond-forming, thus, a five-membered heterocycle with a terminal O–R<sup>2</sup> substituent on a trivalent B center in the ring.<sup>79</sup> Structure 4c is an exception: the O–N bond remains intact, and the ring atoms remain coplanar, but the dative bonding is disrupted—with the B→O separation opening up to lengths >2.0 Å (which, as we confirm shortly, is too long for any significant B←O dative bond). System 5 tended to break apart to release an H–C≡N unit and a chain of the remaining atoms, and system 8 opens up by breaking the O–N bond completely and unfurling in such a manner that B forms a covalent bond to –O–R<sup>2</sup> and becomes trivalent by forming a C=B double bond opposite that B–O bond.

Some of the substituted forms of 1, 2, 3, 6, and 7 also optimized to nonplanar structures as well at the B3LYP level

(Table 1). Cases b, d, and e converged to cyclic minimum energy geometries for series 3, though only d (where R<sup>1</sup> = CH<sub>3</sub> and R<sup>2</sup> = H) remained planar. Case 3a, however, and all of the series 3 species with R<sup>1</sup> or R<sup>2</sup> = CF<sub>3</sub> opened up (at the O→B bond when R<sup>2</sup> = CF<sub>3</sub> and at O–C otherwise).

In the other four promising categories examined (1, 2, 6, and 7; Table 1), the B3LYP planar rings were also disfavored when R<sup>2</sup> = CF<sub>3</sub>; the optimized structures were either distorted nonplanar rings, planar chains with exceptionally long O→B contacts (>2.50 Å, compared to <1.75 Å in other rings), or simple nonplanar molecular chains formed by an opening up of the ring to leave no hint of any O→B interaction (see Table 1). We identify the various cases in Table 1, and we indicate as well particular instances where the hybridization at the oxygen center in 7 is such that the O–H bond (in 7a, 7d, and 7g) is tilted somewhat out of the plane of the ring (see the “.xyz” files provided in the Supporting Information).

Overall, the borylene-like cyclic minimum energy geometries for series 1, 2, 3, 6, and 7 were most stable for cases (a, b, d, e, g, and h) where R<sup>2</sup> = H, or CH<sub>3</sub>. Substituting for the –CF<sub>3</sub> group at the O center is particularly destabilizing for the rings. The substantial polarization of the electron density on O by the electron-withdrawing –CF<sub>3</sub> substituent causes the O lone pair to contract significantly and to become thus much less available for coordination to B. In total, some 28 of the structures were optimized in minimum energy cyclic geometries, and those species are indicated by a tick in Table 1 with a footnote included for cases 3b, 3d, and 3e.

**Borylene Multiplicity.** We have focused so far on singlet systems, and there is a great deal of evidence from simple linear borylenes that the singlet forms tend to be more stable than triplet alternatives,<sup>29,42</sup> though triplet borylenes are not at all unprecedented.<sup>44,54</sup> To assess the multiplicity preferences and the singlet–triplet gaps for all 28 of the optimized cyclic species identified in Table 1, we reoptimized those minimum energy structures as triplets at the same (B3LYP/cc-pVTZ) level of theory (all without any geometrical constraint). Additionally, we reoptimized the singlet B3LYP structures in

**Table 2. Singlet-Triplet  $\omega$ B97XD/cc-pVTZ Free Energy Separations,  $\Delta G_{S-T}(298.15\text{ K}) = G_{\text{singlet}} - G_{\text{triplet}}$ , for Systems with cyclic Singlet and Triplet Minima, Where the Singlet Is a Borylene-Type Species<sup>a</sup>**

	R <sup>1</sup>	R <sup>2</sup>	$\Delta G_{S-T}(298.15\text{ K})/\text{kcal}\cdot\text{mol}^{-1}$				
			1	2	3	6	7
a.	H	H	-2.39	3.32	–	-20.80	-46.80
b.	H	CH <sub>3</sub>	-1.64	3.96	-1.44	-19.23	-46.84
d.	CH <sub>3</sub>	H	-4.58	0.66	-2.95 <sup>c</sup>	-20.05	-45.92
e.	CH <sub>3</sub>	CH <sub>3</sub>	-3.49	1.41	-2.92	-18.35	-46.20
g.	CF <sub>3</sub>	H	0.70	6.56	–	-17.64	-43.46
h.	CF <sub>3</sub>	CH <sub>3</sub>	1.88	7.35	–	-16.38	-43.43
i.	CF <sub>3</sub>	CF <sub>3</sub>	–	10.66 <sup>b</sup>	–	–	–

<sup>a</sup>The singlet–triplet electronic energy difference ( $\Delta E_{S-T}$ ), zero-point corrected values ( $\Delta(E+ZPE)_{S-T}$ ), and enthalpies ( $\Delta H_{S-T}(298.15\text{ K})$ ) as well are included in the Supporting Information. <sup>b</sup>Distorted singlet ring(s) at the  $\omega$ B97XD level. <sup>c</sup>The B←O contact in the triplet is quite long at 1.841 Å, rendering the triplet system essentially an open flat chain.

**Table 3. Singlet–Triplet Energy Separations, ( $\Delta E_{S-T} = E_{\text{singlet}} - E_{\text{triplet}}$ ) for Series 7 Systems Using the Methods Listed along with the cc-pVTZ Basis Set**

	R <sup>1</sup>	R <sup>2</sup>	series 7, $\Delta E_{S-T}/\text{kcal}\cdot\text{mol}^{-1}$						
			B3LYP	B3LYP-D3BJ	M06	M06-2X	$\omega$ B97XD	MP2(full)	CCSD(T) <sup>a</sup>
a	H	H	–	–	–	-46.4	-48.3	-48.8	-51.1
b	H	CH <sub>3</sub>	-46.5	-46.2	-47.0	-44.5	-48.2	-48.2	-49.9
d	CH <sub>3</sub>	H	–	–	–	-45.5	-47.5	-48.1	-50.0
e	CH <sub>3</sub>	CH <sub>3</sub>	-45.8	-45.7	-47.2	-44.2	-47.7	-47.8	-49.2
g	CF <sub>3</sub>	H	-43.4	-43.4	-45.7	-42.4	-44.1	-43.2	-46.5
h	CF <sub>3</sub>	CH <sub>3</sub>	-42.7	-41.9	-44.3	-40.8	-43.9	-42.9	-45.4

<sup>a</sup>Energy calculation on a  $\omega$ B97XD optimized structure.

both the singlet and triplet states using the MP2(full) method and the diverse group of density functional methods (B3LYP-D3BJ, M06, M06-2X, and  $\omega$ B97XD) mentioned in the methods section. The resulting data are included in the Supporting Information (with coordinates in viewable “.xyz” files and energy data in Tables S1–S7). The singlet–triplet (S–T) free energy values ( $\Delta G_{S-T} = G_{\text{singlet}} - G_{\text{triplet}}$ ) obtained at the  $\omega$ B97XD level, which incorporates dispersion in a coherent manner and more fully than the B3LYP method, are included here as well (Table 2).

To afford ourselves and the reader some references for the quality of the MP2(full) and density functional S–T gap data for the rings, we computed S–T gaps as well for the structurally simpler and computationally less demanding :BH, :CH<sub>2</sub>, :NH<sub>2</sub><sup>+</sup>, and :SiH<sub>2</sub> species at the same levels of theory mentioned above and at the CCSD(T)/cc-pVTZ level (see Tables S8–S9). Experimental data are available for those small species (see Table S9)<sup>80–83</sup> and we find that several of the methods that we employed in this work provide S–T gaps comparable to those obtained at the CCSD(T) level and from experiment. Using the experimental data as our reference, we find in fact that the density functional methods consistently outperform the MP2(full) method in this regard. For :NH<sub>2</sub><sup>+</sup>, for instance, with an experimental value of  $30.1 \pm 0.2\text{ kcal}\cdot\text{mol}^{-1}$ <sup>84</sup> and a CCSD(T) value of  $30.6\text{ kcal}\cdot\text{mol}^{-1}$ , the density functional based methods return values within the range  $33.1 \leq \Delta G_{S-T}/\text{kcal}\cdot\text{mol}^{-1} \leq 34.0$  compared to  $36.5\text{ kcal}\cdot\text{mol}^{-1}$  at the MP2(full) level (Table S7).

Returning to the more involved ourboric rings systems, it is clear from the  $\omega$ B97XD data in Table 2, and the results shown in the Supporting Information (Tables S1–S7) for other methods, that several of the systems that we considered have triplet rather than singlet minima. As for the simple cases considered above, the MP2 method noticeably underestimates

in some cases and overestimates in other cases the S–T gaps relative to all of the other methods. This disagreement is especially prominent in cases where the gaps are relatively small, as in the case of series 2 (see Table S7).

Yet (excluding for the moment the MP2(full) values, which return singlet preference in all cases (Tables S6 and S7)), the density functional methods agree that the series 2 systems have triplet ground states (with  $\Delta G_{S-T}$  close to zero in several cases and generally less than  $10\text{ kcal}\cdot\text{mol}^{-1}$ ). And the situation is similar for cases where the R<sup>1</sup> = CF<sub>3</sub> for series 1 (i.e., 1g, and 1h). The other cases for series 1 and 3 are generally found to prefer the singlet state, but with  $|\Delta G_{S-T}| < 5.5\text{ kcal}\cdot\text{mol}^{-1}$  for all of the density functional methods that we employed (Table S7).

The singlet preference is unequivocal, however, and the barriers are far more substantial for series 6 and 7. For the former,  $\Delta G_{S-T}$  is between  $-14$  to  $-21\text{ kcal}\cdot\text{mol}^{-1}$  by the density functional methods, depending on the identities of R<sup>1</sup> and R<sup>2</sup> (Tables 2 and S7), with some augmentation by 5 to 7  $\text{kcal}\cdot\text{mol}^{-1}$  at the MP2 level (Table S7). And the situation is even more remarkable for series 7 (Table 3)!

Those five-membered (series 7) ring systems show by far the strongest preference for the singlet state (and, too, the best agreement between the density functional and MP2(full) methods); with  $-40 > \Delta E_{S-T}/\text{kcal}\cdot\text{mol}^{-1} > -49$  (Table 3; see Table S7 for the corresponding  $\Delta G$  values). We should mention that the optimized triplet ring opens up in two cases (7a, and 7d) for the B3LYP, B3LYP-D3BJ, and M06 methods, but the ring persists in the other cases, and for immediate comparison of the singlet–triplet gaps, we include herein the  $\Delta E_{S-T}$  values (energy gaps without zero-point corrections) for all of the relevant methods (Table 3). For comparison, we include in Table 3 as well the computationally more demanding CCSD(T) S–T energy gaps obtained for the

preoptimized  $\omega$ B97XD structures. Those CCSD(T) energies are consistently a bit larger than the values obtained otherwise, but even in that case, where the energies are between  $-45$  and  $-51$  kcal·mol $^{-1}$  (Table 3), identical trends are observed in the data; The singlet form is strongly preferred in all cases, and  $\Delta E_{S-T}$  is largest for 7a and smallest when  $R_1 = \text{CF}_3$  (7g and 7h in Table 3). Of note, the magnitudes of the S–T gaps achieved by these series 7 oxo-borylenes are surprisingly large compared to that record values of  $\sim -30.0$  kcal·mol $^{-1}$  obtained for (*N*-heterocyclic) borylene rings posited in ref 55 (see Table S10).

**Structure and Bonding.** We focus, henceforth, only on the series 6 and 7 systems. Both series feature a “N–B←O” fragment in the rings, have well-defined closed singlet rings for all of the methods considered, and exhibit by far the largest S–T gaps, with very strong preferences for the singlet multiplicity.

Unless stated otherwise, we include  $\omega$ B97XD quality data in the text, with results from other methods included in some cases in the Supporting Information. We show in Table 4, the

**Table 4. Key ( $\omega$ B97XD/cc-pVTZ) B–N, and B←O Bond Distances of Singlet Borylene Rings for Series 6 and 7, All with B←O  $\leq 1.72$  Å, and the Corresponding Wiberg Bond Orders for B–N and B←O Contacts in Those Rings**

	R <sup>1</sup>	R <sup>2</sup>	bond distances, <i>r</i> /Å			
			B–N		B←O	
			6	7	6	7
a	H	H	1.461	1.442	1.610	1.714
b	H	CH <sub>3</sub>	1.458	1.447	1.628	1.638
d	CH <sub>3</sub>	H	1.467	1.444	1.596	1.685
e	CH <sub>3</sub>	CH <sub>3</sub>	1.464	1.449	1.613	1.623
g	CF <sub>3</sub>	H	1.485	1.470	1.588	1.630
h	CF <sub>3</sub>	CH <sub>3</sub>	1.483	1.472	1.600	1.594
	R <sup>1</sup>	R <sup>2</sup>	Wiberg bond orders, <i>N</i>			
			B–N		B←O	
			6	7	6	7
a	H	H	0.853	0.921	0.465	0.407
b	H	CH <sub>3</sub>	0.852	0.920	0.441	0.443
d	CH <sub>3</sub>	H	0.813	0.887	0.478	0.427
e	CH <sub>3</sub>	CH <sub>3</sub>	0.807	0.882	0.452	0.452
g	CF <sub>3</sub>	H	0.784	0.826	0.479	0.465
h	CF <sub>3</sub>	CH <sub>3</sub>	0.779	0.821	0.457	0.472

computed B←O bond distances for the optimized series 6 and 7 ring structures. To be clear, we focus only on systems with short B←O dative contacts ( $<1.75$  Å in Table 4)—systems in which the geometries imply substantial charge transfers between the O and B centers in the ring—and that criterion is satisfied by all of the singlet rings that we have located for both series 6 and 7.

For comparison with the structural data in Table 4, the geometries of several simple complexes of small mono and trivalent boron species (all optimized at the same ( $\omega$ B97XD/cc-pVTZ) level) are reported in the Supporting Information (Figure S1). The covalent B–C, B–N, and B–O bonds in the simple molecules H<sub>2</sub>B–CH<sub>3</sub>, H<sub>2</sub>B–NH<sub>2</sub>, and H<sub>2</sub>B–OH are 1.554, 1.387, and 1.349 Å, respectively. The short B–N and B–O bond distances in those small reference molecules compared to the B–C contact are explained of course not only by the smaller atomic radii for N and O relative to C but also by a significant double bond character in those B–N and B–O contacts due to  $\pi$ -delocalization from N and O into the empty

*p* orbital on boron. And that distinction from the B–C bond is reflected too in slightly higher Wiberg bond orders (*N*), which are  $N_{\text{B–C}} = 0.98$ ,  $N_{\text{B–N}} = 1.3$ , and  $N_{\text{B–O}} = 1.1$ . In contrast, the B–N and B–O bonds in classical dative complexes H<sub>3</sub>B←NH<sub>3</sub>, and H<sub>3</sub>B←OH<sub>2</sub> (Figure 2a,b) are noticeably longer 1.647 and 1.719 Å, respectively, with much smaller bond orders:  $N_{\text{B←N}} = 0.66$  and  $N_{\text{B←O}} = 0.46$ .

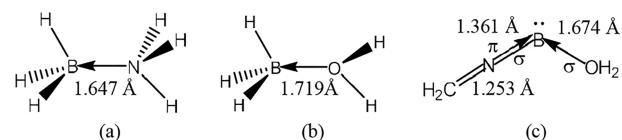


**Figure 2.** Reference structures with dative  $\sigma$  B–O bonding and (in part c)  $\pi$ -delocalization, to tri- and monovalent B centers (see  $\omega$ B97XD structures in Figure S1). The bond energies ( $E(\text{complex}) - E(\text{base}) + E(\text{acid})$ ) are  $-33.2$  (B←N),  $-16.6$  (B←O), and  $-5.7$  (B←O) in kcal/mol units.

Compared to the H<sub>3</sub>B←OH<sub>2</sub> dative bond, however, an acyclic bonding arrangement that more closely approximates the bonding arrangement at the B center in series 6 and 7 structures is the model borylene structure shown in Figure 2c.

In that system, the borylene center is covalently bonded to a nitrogen atom and forms a dative B←O bond, which has a computed ( $\omega$ B97XD) bond length of 1.674 Å and a Wiberg bond order of 0.42 (compare to 1.719 Å and 0.46 for H<sub>3</sub>B←OH<sub>2</sub>). That system in Figure 2c lacks both the constraints, cyclic arrangement, and putative cyclic  $\pi$ -delocalization of the series 6 and 7 structures, but unlike H<sub>3</sub>B←OH<sub>2</sub>, it combines both the covalent B–N  $\sigma$  bond and the B←N  $\pi$  delocalization (likely with some however weaker B←O  $\pi$  contribution as well, though that is not depicted in Figure 2c).

Incidentally, the short B–N contact in the complex in Figure 2c (1.361 Å), has a bond order in excess of unity ( $N_{\text{B–N}} = 1.2$ ), and the recovery of a B–N double bond and a lone pair on B from an NBO analysis (using the NBO 3.1 program as implemented in G09<sup>63</sup>) supports the claim that some  $\pi$ -bonding is at work in stabilizing the system, as we expect to be the case as well in the cyclic series 6 and 7 structures. Along with the B–N and B←O bond distances, the corresponding Wiberg bond orders in series 6 and 7 ring structures are also included in Table 4. The B–N bonds in the rings are longer (by as much as 0.12 Å) and the bond orders are smaller (by up to 0.4) compared to the model chain complex in Figure 2c (where  $r_{\text{B–N}} = 1.361$  Å and  $N_{\text{B–N}} = 1.2$ ). This suggests that the extent of any reinforcement of the  $\sigma$  bonding in the ring by  $\pi$ -delocalization may be somewhat lower for series 6 and 7 structures than it is in the acyclic system in Figure 2c.

The B←O bonds in the borylene rings (Table 4) are all shorter than the dative bond to the trivalent B center in H<sub>3</sub>B←OH<sub>2</sub> (Figure 2b), but they are more comparable to the B←O bond in the acyclic borylene species in Figure 2c. As a point of comparison,  $r_{\text{B←O}} = 1.685$  Å and  $N_{\text{B←O}} = 0.43$  for structure 7d (Table 4) and  $r_{\text{B←O}} = 1.674$  Å and  $N_{\text{B←O}} = 0.42$  for the structure in Figure 2c.

As is typical, the bond orders vary indirectly with bond distance in both series 6 and 7. This is apparent from a comparison of *N* and *r* in Table 4 and from the graphs of *N* vs *r* in Figure S2. A closer analysis of the relationship between  $r_{\text{B←O}}$  and  $N_{\text{B←O}}$  is provided in the Supporting Information to preserve here the focus on the structure and frontier electron

distribution in the rings. We should point out here, however, that in addition to the  $N$  and  $r$  data in Table 4, we expanded the data set by computing and including in that graph of  $N$  vs  $r$  (Figure S2) cases where  $R^1 = \text{F, Cl, Br, OH, CN, and COH}$  as well for  $R^2 = \text{H, or CH}_3$  (see Table S11). We exclude  $R^2 = \text{CF}_3$  since, as we pointed out above, no stable cyclic form was obtained at all for any series 6 or 7 structure with the  $\text{CF}_3$  substituent on O.

That larger  $N$  vs  $r$  data set falls rather neatly into categories on the graph (Figure S2) based on the identity of  $R^2$ , and we have added best-fit lines of the form  $N = A \cdot r^{-b}$  along with the corresponding equations and coefficients of determination. That functional form was considered and employed here since it matches the data set well and is in line with the functions proposed by Gordy and others for covalent bonds,<sup>85,86</sup> but it has not been applied before for ouroboric dative bonds. That inverse form, where  $N$  is the bond order and  $r$  is the bond distance suits as well the chemical meanings of  $N$  and  $r$ ;  $N$  is always positive over the range of possible  $r$  values, and it moves rapidly to zero as  $r$  increases.

**Borylenic Character of the Rings.** NBO analyses performed on the optimized ring systems recover unequivocally the anticipated lone pair on B, each with the substantial occupancies shown in Table 5. The existence of a lone pair on

**Table 5. Populations for the Lone Pair on B in the Singlet Cyclic Borylene Systems**

	$R^1$	$R^2$	lone pair orbital populations	
			6	7
a	H	H	1.95	1.94
b	H	$\text{CH}_3$	1.94	1.93
d	$\text{CH}_3$	H	1.95	1.94
e	$\text{CH}_3$	$\text{CH}_3$	1.93	1.93
g	$\text{CF}_3$	H	1.95	1.93
h	$\text{CF}_3$	$\text{CH}_3$	1.93	1.93

the borylene center is expected based on the Lewis structures shown in Figure 1, but the results in Table 5 quantify the extent of the orbital localization, and we show in Figure 3 the key canonical frontier orbital that is dominated by the lone pair.

The figure features, for each optimized ring in series 6 and 7, the molecular orbitals in which the bulk of the electron density is concentrated primarily at the boron site away from the ring. For all of the series 6 and 7 ring structures, this orbital turns

out to be the highest occupied molecular orbital (HOMO). The fact that the lone pair is the HOMO of the molecule indicates that in these neutral cyclic borylenes this lone pair is the site in the molecule that will be most readily engaged in reactions by direct attack by electrophiles. The reactivity of the rings is not examined in detail in this work, and some distribution of the lone pair electron density from B onto the adjacent carbon center is a characteristic of all of the rings (Figure 3), but the substantial localization of the electron density on the B center for these systems is clear from Figure 3 and from the high (lone pair) orbital occupancies in each case (Table 5).

#### Aromaticity in Ouroboric B←O Cyclized Borylenes.

All 72 of the singlet ring systems represented in Figure 1 have resonance forms that allow potentially for  $\pi$ -electron delocalization. For series 6 and 7, this would involve a combination of lone pairs on O and N that are perpendicular to the plane of the ring, and the electrons of the  $\text{C}=\text{C}$  double bond shown in the resonance structures for 6 and 7 in Table 1 and Figure 3. It is already clear from our results for series 1 to 8 that the specific position of the heteroatoms in the ring and the nature of  $R^1$  and  $R^2$  are decisive for the stability and planarity of the ring, and will influence the extent of any  $\pi$ -electron delocalization in them as well. Given that the singlet state is an excited state for all of the series 2 and some of the series 1 ring structures and that there is only a marginal bias toward the singlet form for other cyclic species in series 1 and 3, we wanted to look more closely at the potential roles of aromaticity in motivating the far greater preference for the singlet state that we observe here for series 6 and 7.

We have not located any other investigation of ouroboric borylene rings closed by B←O bonds. So, although high symmetry is not necessary for  $\pi$ -delocalization, and all of the series 6 and 7 rings are planar (except that the terminal O–H bond in 7a, 7d, and 7g each tilt somewhat out of the plane of the ring), the extent of any aromaticity in the rings and the potential impact on structural stability remains unclear.

We employed two strategies for estimating the aromatic character of the systems: the isomerization stabilization energy (ISE) method for assessing aromatic stabilization energies (ASE)—a suggestion from a reviewer—and the nucleus independent chemical shifts (NICS<sub>zz</sub>).

**Aromatic Stabilization Energy Analysis.** The isomerization stabilization energy (ISE) method for computing aromatic stabilization energies<sup>72</sup> assesses aromaticity by disrupting the presumed  $\pi$  delocalization in a methyl-substituted unsaturated ring by an isodesmic methyl-

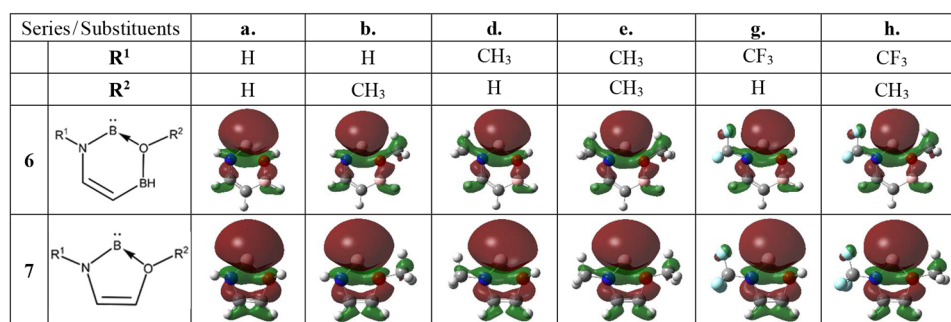


**Figure 3.** Semitransparent representations of the frontier molecular orbitals in the singlet rings for series 6 and 7 (each, incidentally, the HOMO) that is dominated by the lone pair on B (the orbital pictures are oriented in the same ways as the structures shown on the far left above, with B at the top and the O center on the right).

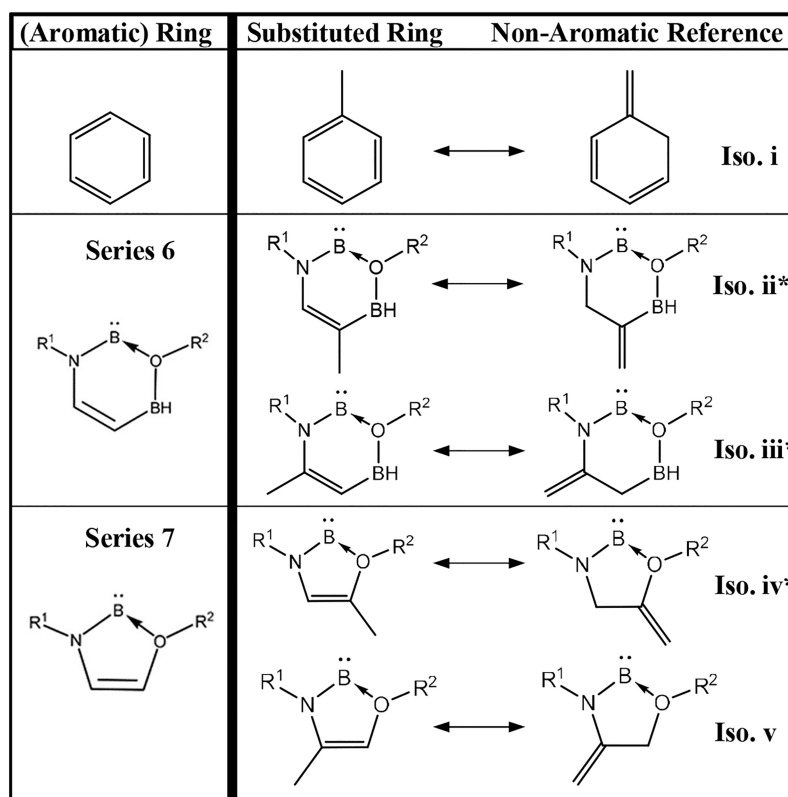


**Figure 4.** Structural isomers considered for assessing aromatic stabilization energies (ASE) in singlet rings using the isomerization stabilization energy (ISE) method. In several cases,\* substitution and disruption of  $\pi$ -bonding in the ring, in the methylene isomers, led to ring opening.

methylene rearrangement that saturates a point on the ring. A negative energy difference between the unsaturated ring and its locally saturated isomer (by the definition,  $\Delta E_{ASE} = E_{methyl} - E_{methylene} < 0$ ) implies some degree of aromatic stabilization of the former. A simple example using benzene is shown at the top in Figure 4, and we include in the figure the isomers that we assessed for series 6 and 7 as well.

In each case, the two isomers considered are an (ostensibly) aromatic, methyl-substituted, ring and the nonaromatic methylene form. Unlike the benzene case, series 6 and 7 structures are unsymmetrical, so we had to consider both substitution options about the C=C double bond.

This methyl-to-methylene isomerization is a structurally invasive strategy for assessing aromaticity; however, it mandates a degree of rehybridization at atomic centers (introducing an  $sp^3$  C and an *exo*-double bond on the far right in Figure 4) and associated changes in the strain, interatomic separations, and electron distribution in the ring. For a covalently bound ring such as benzene, those changes do not substantially compromise the integrity of the ring, but—as it turns out—they can for our boron rings. For the rings closed by B←O dative bonds in Figure 4, the substitutions are destabilizing for several of the rings, especially for the series 6 compounds.

In both cases for series 6 (isomerization (Iso.) ii and iii in Figure 4), the methyl-substituted rings remain planar and closed, but the methylene forms open up at the B←O bond and planarity is typically sacrificed as well as the system relaxes to a new minimum energy chain geometry. It was not possible therefore to meaningfully assess ASE value for those species. Without setting out to do so, therefore, our efforts here demonstrate limitations to invasive strategies for assessing

aromaticity in the cases where the  $\sigma$  framework is supported by dative bonds (or even weaker interactions potentially such as hydrogen or halogen bonds). More critically perhaps, it highlights as well the challenge with preparing cyclic dative species (including but not limited to borylenes) and modifying them even at sites on the ring that are far from the site of the actual dative bond.

For Series 7, a similar outcome is observed for the methylene forms for Iso. iv, except for the cases where  $R^1 = CF_3$ . For Iso. v in Figure 4, however, where the methyl/methylene substitution is one carbon away from the N center, all of the rings optimized as planar cyclic structures with short B←O contacts ( $\leq 1.72$  Å), and the data are summarized in Tables 6 and S12.

For an aromatic system, the expectation is that the value will be negative by the definition we have used here for ASE,<sup>72</sup> with increasingly positive values as we move to a nonaromatic arrangements and large positive values for unambiguously antiaromatic cases (see the ASE values for benzene and cyclobutadiene in Table 6). Our results in Table 6 indicate thus that system 7 may be slightly aromatic—though only marginally so relative to benzene. The asymmetry of the electron density is reflected in the sensitivity of both the ASE values and the stability of the substituted rings themselves to the position (Iso. iv vs v) of the methyl/methylene substitutions. The stability of these B←O cyclized borylenes is quite sensitive to the composition of the rings, including local substitutions, and we say more shortly about potential roles for electron-withdrawing and -donating groups for maintaining or enhancing ring stability in these borylenes.

**NICS Analysis.** As we mentioned in methods section, NICS<sub>zz</sub> data are a useful indicator of aromaticity, especially

**Table 6.** ( $\omega$ B97XD/cc-pVTZ) Aromatic Stabilization Free Energies ( $ASE = E_{\text{methyl}} - E_{\text{methylene}}$ ) for Isomerizations Depicted in Figure 4 Where both the Optimized Methyl and Methylene Forms Are Borylene Rings

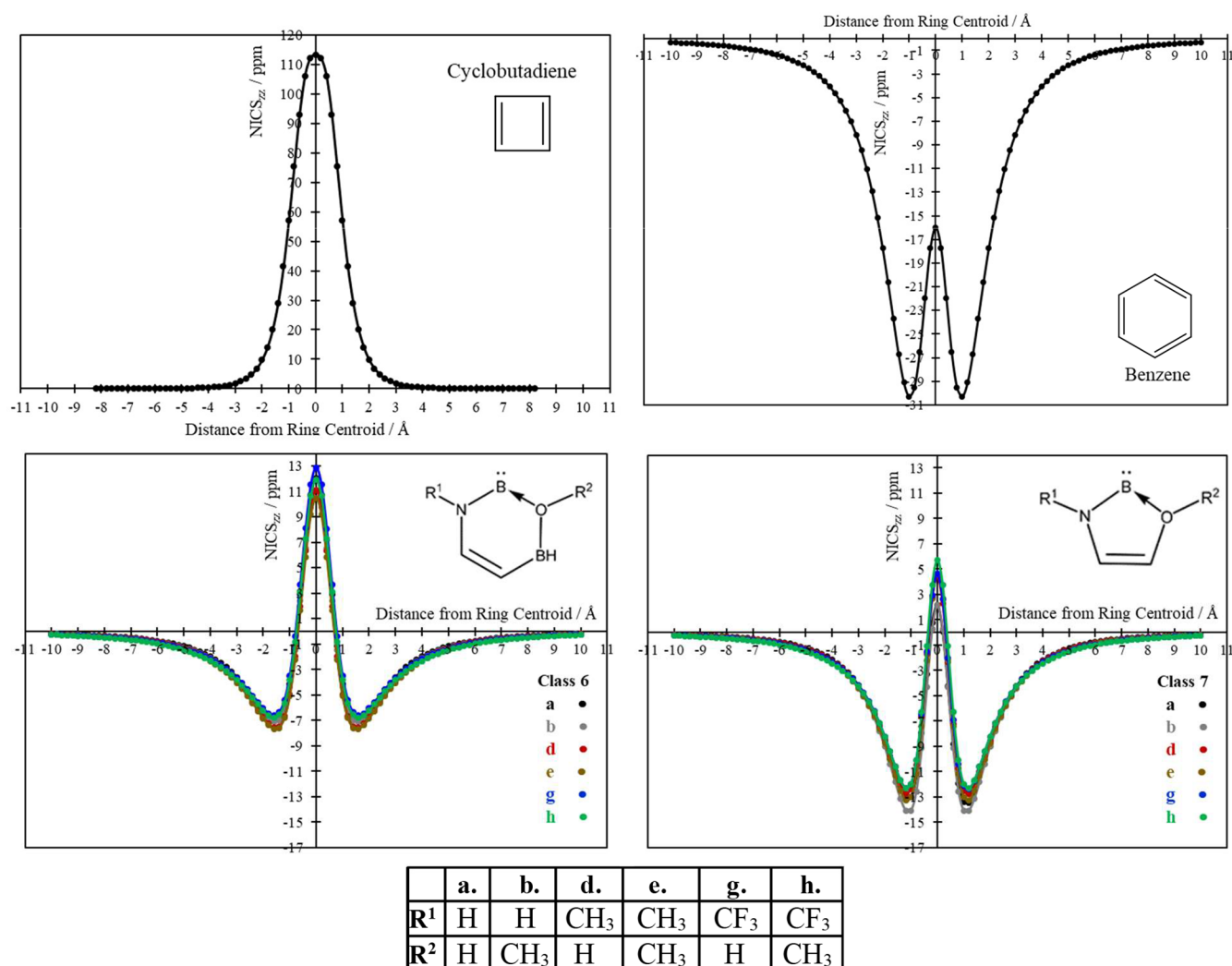
	R <sup>1</sup>	R <sup>2</sup>	methylene $\rightarrow$ methyl ASE/kcal·mol <sup>-1</sup>	
			7 (Iso. (iv)) <sup>a</sup>	7 (Iso. (v))
a	H	H	–	–2.5
b	H	CH <sub>3</sub>	–	–3.1
d	CH <sub>3</sub>	H	–	–0.9
e	CH <sub>3</sub>	CH <sub>3</sub>	–	–1.4
g	CF <sub>3</sub>	H	–5.7 <sup>b</sup>	–3.2
h	CF <sub>3</sub>	CH <sub>3</sub>	–4.7	–3.7
benzene			–34.8 <sup>c</sup>	
cyclobutadiene			34.1	

<sup>a</sup>In several cases, the methylene substituted structure optimized to a nonplanar borylene chain. <sup>b</sup>The methylene substituted structure for “Iso. iv” g optimizes as a ring, but with a rather long B←O distance of 1.727 Å. <sup>c</sup>This benzene value has been corrected for the so-called *anti-syn* diene mismatch by adding the difference in energy between the 2-methyl-1,3-cyclohexadiene (*syn*) and 3-Methylenecyclohexene (*anti*) as prescribed in ref 72.

when considered along an extension beyond the center of the ring rather than at an isolated point at the center of or above the ring. We have computed and plotted for all of the optimized ground state singlet rings for systems 6 and 7 the *z*-components of the nucleus independent chemical shifts (NICS<sub>zz</sub>) (see Figures 5 and S3).

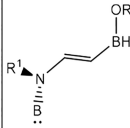
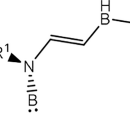
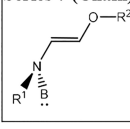
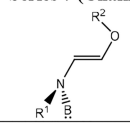
For each system, the *x*–*y* plane contains the centroid and average positions of the five or six atoms in the ring, and the *z*-direction is perpendicular to that plane. The NICS<sub>zz</sub> curves are plotted from the centroid through to 10 Å above and below each ring in 0.2 Å intervals. The bidirectional assessment is redundant for completely planar species, but it is necessary for planar rings with out-of-plane or polyatomic substituents—including 7a, 7d, and 7g where the O–H bond is not in the plane of the ring. Yet, we can already confirm (see Figure 5) that this out-of-plane displacement of the terminal O–H bond or other such features has relatively little impact on the symmetry of the NICS<sub>zz</sub> curves. For comparison with the borylene data, we include in Figure 5 the NICS<sub>zz</sub> curves for both benzene and cyclobutadiene, quintessential examples of aromatic and antiaromatic compounds, respectively.

The series 6 structures each yield nearly identical NICS<sub>zz</sub> curves, all consistent with weakly- to nonaromatic character.



**Figure 5.** ( $\omega$ B97XD/cc-pVTZ) NICS<sub>zz</sub> plots for cyclobutadiene, benzene, and optimized singlet rings of 6 and 7.

Table 7. (wB97XD/cc-pVTZ) Energy, and Free Energy Differences,  $\Delta G_{\text{chain} \rightarrow \text{ring}}(298.16\text{K}) = G_{\text{ring}} - G_{\text{chain}}$  between the Reference Borylene Chains<sup>a</sup> and the Ring, Where All Values Are in kcal·mol<sup>-1</sup>

		a	b	d	e	g	h			a	b	d	e	g	h
R <sup>1</sup> →		H	H	CH <sub>3</sub>	CH <sub>3</sub>	CF <sub>3</sub>	CF <sub>3</sub>	R <sup>1</sup> →		H	H	CH <sub>3</sub>	CH <sub>3</sub>	CF <sub>3</sub>	CF <sub>3</sub>
R <sup>2</sup> →		H	CH <sub>3</sub>	H	CH <sub>3</sub>	H	CH <sub>3</sub>	R <sup>2</sup> →		H	CH <sub>3</sub>	H	CH <sub>3</sub>	H	CH <sub>3</sub>
Series 6 (Chain) <sup>a</sup> 	$\Delta E$	-5.18	-6.17	-3.85	-4.69	-4.40	-5.24	Series 6 (Chain) <sup>b</sup> 	$\Delta E$	-2.54	-2.32	-3.20	-3.43	-4.19	-4.08
	$\Delta G$	-0.87	-1.89	-0.77	-1.60	-1.35	-2.44		$\Delta G$	0.76	0.85	-0.11	-0.42	-1.25	-1.34
Series 7 (Chain) <sup>a</sup> 	$\Delta E$	0.52	-2.33	1.83	-1.02	0.87	-2.55	Series 7 (Chain) <sup>b</sup> 	$\Delta E$	1.09	-0.75	2.44	0.59	1.52	-0.73
	$\Delta G$	2.06	-0.23	3.10	0.65	1.84	-0.91		$\Delta G$	2.40	0.24	3.46	1.06	2.29	-0.37

<sup>a</sup>Key: (a) Chains generated by optimizing the *E* isomer (obtained by breaking the dative B←O bond and rotating about the C=C double bond in the ring). (b) Alternative chains optimized starting from an isomer modified by a reorientation at the O end of the chain.

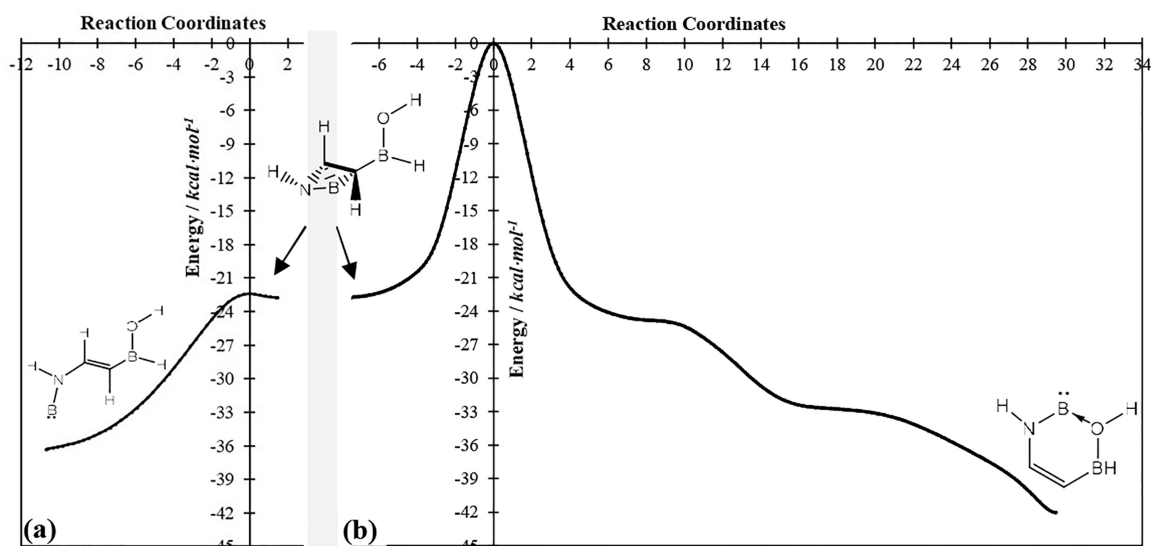


Figure 6. Combination of two internal reaction coordinate (IRC) paths that, together, take us from the ouroboric ring (IRC (b) on the right) to a simple chain (IRC (a) on the left) for singlet structure **6a**. The end of one IRC path and the start of the other is the same shallow intervening minimum. The higher transition structure is used as the reference ( $E = 0$ ).

The profiles for this set of molecules are midway between those of cyclobutadiene and aromatic benzene, but with negative NICS<sub>zz</sub> values at and beyond 1 Å, and an extremum at  $\sim -7$  ppm compared to  $-30$  ppm for benzene. A substantial modification to **6**, however—i.e. eliminating the B–H fragment, which increases ring strain but reduces the ring size without changing the  $\pi$ -electron count—gives system **7**, and enhances aromaticity noticeably. Those planar five-membered ring structures (system **7**; Figure 5), exhibit by far the greatest degree of singlet stability of all of the rings that we considered (see Tables 2 and 3), and are unequivocally—to the extent that the NICS<sub>zz</sub> is an adequate measure—the most aromatic singlet cyclic borylenes identified in this work.

To date, no isolated cyclic borylene has been prepared experimentally—neither singlet nor triplet, neutral, or otherwise. We consider some of the species examined and proposed herein to be worthy candidates for consideration as possible synthetic targets in the exploration for stable aromatic singlet borylenes. Of note, the system **7** singlet bonding motif, though strained and sensitive to substituent choice, manages in

several cases a massive singlet–triplet gap and offers up some evidence of aromatic stabilization as well (Figure 5).

#### Other Considerations I: Competing Chain Forms.

There are many possible local chain-type isomers that can be envisioned for the ouroboric rings considered here, if the dative B←O bond is disrupted. One such isomer may be generated for series **6** and **7** structures by breaking the dative bond and carrying out a *Z* to *E* isomerization about the C=C double bond. We do not undertake an exhaustive scan of the potential energy surface, but we consider here the ring formation energy starting from that *E* isomer (on the left in Table 7) as well as another case that is a simple chain rotomer (on the right in Table 7; with coordinates included in the Supporting Information), and the resulting energies are shown in Tables 7 and S13.

We find that the rings are generally separated from the unstrained chains by a few kcal·mol<sup>-1</sup>, with differences in the relative stability of the chain and the ring depending on the identities of R<sup>1</sup> and R<sup>2</sup>. Notable, there is a general preference for the ring form for series **6**. As we noted at the outset,

**Table 8. Impact of Bulky Substituents on Bond Distances (in Å Units Obtained at the ( $\omega$ B97XD/cc-pVTZ) Level) in Series 6 and 7 Singlet Rings<sup>a</sup>**

	R <sup>1</sup>	F	CF <sub>3</sub>	CH <sub>3</sub>	<i>tert</i> -butyl	Ph	H	Ph
	R <sup>2</sup>	<i>tert</i> -butyl	<i>tert</i> -butyl	<i>tert</i> -butyl	<i>tert</i> -butyl	<i>tert</i> -butyl	<i>tert</i> -butyl	Ph
series 6	B–N	1.445	1.474	1.456	1.470	1.467	1.448	1.471
	B←O	1.571	1.605	1.649	1.588	1.624	1.669	1.674
series 7	B–N	1.438	1.465	1.440	1.371	1.380	1.381	1.408
	B←O	1.615	1.612	1.682	(3.223) <sup>a</sup>	(3.164) <sup>a</sup>	(2.809) <sup>a</sup>	(2.637) <sup>a</sup>

<sup>a</sup>Certain structures open up at the B←O bond (“Open” is defined here as having a B...O separation in excess of  $\sim 1.75$  Å, especially—as is the case here—if that structure is so distorted as well that planarity is lost.).

however, several of the ring motifs considered (such as series 5 and 8) are quite unstable relative to chain forms. For the series 7 systems, the rings are competitive minima, but **7h**—with the electron-withdrawing R<sup>1</sup> and electron-donating R<sup>2</sup> fragments (CF<sub>3</sub> and CH<sub>3</sub>, respectively)—is the only case for that series where ring formation is exergonic relative to the chain isomers considered.

We have been unable to trace (in a single transit) complete paths from the chain forms to the rings by internal reaction coordinate (IRC)<sup>87,88</sup> analyses, even for series 6, because of the high barrier to rotation about the double bond and intervening chain-like minima associated with other rotations about other single bonds in the chains. We have had success, however, in assessing the nature of the barriers separating the simplest series 6 ring, **6a**, from a shallow local minimum en route to a chain form (far left in Figure 6) and, separately, the rest of the path from that local minimum to the ring (far right Figure 6).

IRC calculations typically do not afford a full optimization of the end points on the paths, so the relative energies of the transition structures of both IRCs are used to position the curves on the graphs, using the higher energy transition structure as reference ( $E = 0$  in Figure 6). The final chain structure on the left in Figure 6 is indeed to the *E* isomer for **6a** on the left in Table 7. So, the ring formation or cyclization energy computed for **6a** ( $-5.18$  kcal·mol<sup>-1</sup> in Table 7) is consistent with the energy difference between the chain and ring ends of the composite energy profile in Figure 6.

**Other Considerations II: Bulkier Substituents.** A reviewer asked, not unreasonably, about a possible role for bulky substituents. It is well-known that bulky substituents can protect carbenes and other weaker or potentially reactive centers in molecules, such as dative bonds. We know that for certain Arduengo carbenes, bulk is not crucial to stability,<sup>89</sup> but no information is available on that count yet for our boronic cyclic borylenes such as those introduced here, and we have already pointed out in previous sections the relative sensitivity of some of the series 6 and 7 rings to perturbations, even to local substitutions. We have examined thus a number of substituted series 6 and 7 rings, all confirmed as minima through vibrational frequency analyses, with bulkier (*tert*-butyl, and phenyl) substituents at the R<sup>1</sup> or R<sup>2</sup> positions (Table 8). We identified earlier the need for electron-donating substituents at R<sup>2</sup> for ring stability, hence our choice of the *tert*-butyl group. But we consider the less electron-donating  $-Ph$  group as well, and we use the chance to assess too the influence of the simple electron-withdrawing F substituent at R<sup>1</sup>.

An investigation of reactivity warrants a separate investigation, but our results reveal a simple pattern for the extent of the dative bonding in the rings. Namely, (i) for a given pair of substituents, the less strained six-membered ring (series 6)

leads to shorter B←O contacts and more significant B←O bonding (cf. Tables 4 and S11), (ii) steric repulsion between bulky groups is more consequential and potentially disruptive for the five membered rings, and even in the absence of such effects, (iii) the cyclization of the B←O ourboric borylenes are favored by the presence of a strong  $\sigma$ -acceptor (electron-withdrawing) R<sup>1</sup> substituent (such as R<sup>1</sup> = F or CF<sub>3</sub> in Table 8) and a strong  $\sigma$ -donating R<sup>2</sup> substituent on O on the base side of the ring. These patterns are evident in the opening up of the rings here for series 7 (Table 8) when the bulky electron donating *tert*-butyl or  $-Ph$  groups are at both R<sup>1</sup> and R<sup>2</sup> positions on the series 7 ring (R<sup>1</sup>↔R<sup>2</sup> steric repulsion and the absence of a sufficiently strong electron-withdrawing R<sup>1</sup> substituent at N evidently outstrips any benefit from having the strong  $\sigma$ -donating *tert*-butyl fragment at R<sup>2</sup>).

In brief, series 6 is the more resilient of the two bonding motifs, with relatively short B←O contacts in each case. The quite short B←O bond for R<sup>1</sup> = R<sup>2</sup> = *t*-butyl for series 6 is an anomaly, but otherwise the shortest dative bonds are obtained when R<sup>1</sup> = F and CF<sub>3</sub>, and R<sup>2</sup> = *t*-butyl; the electron-withdrawing R<sup>1</sup> substituents favor cyclization and strong bonding in these ring systems. In both series 6 and 7, substitution on O for “R<sup>2</sup>” groups that are weak donors (on the right in Table 8) is universally destabilizing for bonding, leading to noticeably longer bonds in series 6 and a complete unraveling of the ring in some cases for series 7.

Overall, we find that both series 6 and 7 rings show promise as motifs for stable cyclic borylenes, but R<sup>1</sup> and R<sup>2</sup> must be selected carefully to ensure ring persistence and favorable thermodynamic profiles.

## ■ SUMMARY AND OUTLOOK

Classes of neutral five- and six-membered cyclic borylenes (rings with a boron(I) center), each with six  $\pi$ -electrons in analogy to the cyclopentadienyl anion and benzene, have been proposed and examined. In each case, ring closure is achieved formally by the donation of an oxygen lone pair into one of the two empty orbitals on the monovalent boron center. The outcome is a ring with a Hückel number of  $\pi$ -electrons, with the dative B←O bond reinforced to some modest extent at best by  $\pi$ -delocalization. One instance is the  $:B-NR^1-CH=CH-OR^2$  ring (by one view, a modification of 1,3 oxazole) in which the monovalent boron center is covalently bound to N while accepting a lone pair from the O to form a five-membered ring with terminal substituents R<sup>1</sup> and R<sup>2</sup> on N and O, respectively (see Figure 1).

The presence and position of heteroatoms in the ring, and the identity of R<sup>1</sup> and R<sup>2</sup> are shown to be critical for the stability and planarity of the rings. Of 72 five and six-membered ring species examined, 28 minimum energy singlet

borylene rings have been located. The cases where  $R^1/R^2 = H$  or  $CH_3$  are the favorable substitution patterns across several different ring motifs.  $R^1 = CF_3$  and  $R^2 = CH_3$  in which the electron donor is on the O center is quite favorable as well. Where  $R^2 = CF_3$  or some other strong electron-withdrawing substituent is on O, cyclization is frustrated in almost every case. Equations of the form  $N = A \cdot r^{-b}$ , a dative analogue of Gordy's equation,<sup>85</sup> give excellent fits for the Wiberg bond orders,  $N$ , as functions of the B←O bond distances,  $r$ , in the rings.

In a number of cases, triplet rings are found to be more stable than their singlet ring counterparts. Yet, the most remarkable singlet–triplet gaps ( $|\Delta E_{S-T}| > 40.0 \text{ kcal}\cdot\text{mol}^{-1}$ ) are observed for the five membered rings mentioned above, which prefer the singlet state and exhibit as well some degree of aromaticity. This is so, even as strain and the weakness of dative bonding in those ring (i.e., relative to both a six-membered ourboric ring and fully covalent rings such as benzene) makes cyclization quite sensitive to the position and identity of substituents.

Our results suggest that there is some hope yet for ourboric boron analogues of carbenes. What remains to be uncovered is an effective synthetic route to such systems. The preparation of ourboric borylene species would represent a grand leap beyond the small gas-phase free borylenes that have already been identified.<sup>26,35</sup> The final word on the accessibility of the systems considered in this work and elsewhere,<sup>55</sup> must come, thus, from experimental exploration.

## ■ ASSOCIATED CONTENT

### SI Supporting Information

The Supporting Information is available free of charge at <https://pubs.acs.org/doi/10.1021/acs.jpca.2c04249>.

Models of simple dative complexes and molecules with B–C, B–N, and B–O bonds, graphs of Wiberg bond order vs bond distances, and NICS<sub>zz</sub> plots (PDF)

.xyz files with viewable Cartesian coordinates, supporting notes, and thermodynamic data for compounds examined (ZIP)

## ■ AUTHOR INFORMATION

### Corresponding Author

Kelling J. Donald – Department of Chemistry, Gottwald Center for the Sciences, University of Richmond, Richmond, Virginia 23173, United States; [orcid.org/0000-0001-9032-4225](https://orcid.org/0000-0001-9032-4225); Phone: 1-804-484-1628; Email: [kdonald@richmond.edu](mailto:kdonald@richmond.edu)

### Authors

Ulrick R. Gaillard – Department of Chemistry, Gottwald Center for the Sciences, University of Richmond, Richmond, Virginia 23173, United States

Noah Walker – Department of Chemistry, Gottwald Center for the Sciences, University of Richmond, Richmond, Virginia 23173, United States

Complete contact information is available at: <https://pubs.acs.org/doi/10.1021/acs.jpca.2c04249>

### Author Contributions

<sup>†</sup>U.R.G. and N.W. contributed equally.

### Notes

The authors declare no competing financial interest.

## ■ ACKNOWLEDGMENTS

Our work was supported by the National Science Foundation (NSF-RUI Award (CHE-2055119) and NSF-MRI Grants (CHE-0958696 (University of Richmond (UR)) and CHE-1662030 (the MERCURY consortium). U.R.G. thanks the NSF for a postbaccalaureate research fellowship and U.R.G. and N.W. thank the University of Richmond for summer research support. K.J.D. acknowledges as well the support of the Henry Dreyfus Teacher-Scholar Awards Program.

## ■ REFERENCES

- (1) Ramsey, B. G.; Anjo, D. M. Naphthylboryne: a Monovalent Organoboron Carbene Analogue from Photolysis of Tri-1-naphthylboron. *J. Am. Chem. Soc.* **1977**, *99*, 3182–3183.
- (2) Segawa, Y.; Yamashita, M.; Nozaki, K. Boryllithium: Isolation, Characterization, and Reactivity as a Boryl Anion. *Science* **2006**, *314* (5796), 113–115.
- (3) Romeo, L. J.; Kaur, A.; Wilson, D. J. D.; Martin, C. D.; Dutton, J. L. Evaluation of the  $\sigma$ -Donating and  $\pi$ -Accepting Properties of N-Heterocyclic Boryl Anions. *Inorg. Chem.* **2019**, *58*, 16500–16509.
- (4) Igau, A.; Grutzmacher, H.; Baceiredo, A.; Bertrand, G. Analogous  $\alpha,\alpha'$ -Bis-Carbenoid Triply Bonded Species: Synthesis of a Stable  $\lambda^3$ -Phosphinocarbene- $\lambda^5$ -Phosphaacetylene. *J. Am. Chem. Soc.* **1988**, *110*, 6463–6466.
- (5) Arduengo, A. J., III; Krafczyk, R. Auf der Suche nach Stablen Carbenen. *Chem. Unserer Z.* **1998**, *32*, 6–14.
- (6) Arduengo, A. J. Looking for Stable Carbenes: The Difficulty in Starting Anew. *Acc. Chem. Res.* **1999**, *32*, 913–921.
- (7) Arduengo, A. J.; Harlow, R. L.; Kline, M. A Stable Crystalline Carbene. *J. Am. Chem. Soc.* **1991**, *113*, 361–363.
- (8) Pianalto, F. S.; O'Brien, L. C.; Keller, P. C.; Bernath, P. F. Vibration-Rotation Spectrum of BH X<sup>1</sup>  $\Sigma^+$  by Fourier Transform Emission Spectroscopy. *J. Mol. Spectrosc.* **1988**, *129*, 348–353.
- (9) Brazier, C. R. Emission Spectroscopy of the Triplet System of the BH Radical. *J. Mol. Spectrosc.* **1996**, *177*, 90–105.
- (10) Lovas, F. J.; Johnson, D. R. Microwave Spectrum of BF. *J. Chem. Phys.* **1971**, *55*, 41–44.
- (11) Cazzoli, G.; Cludi, L.; Degli Esposti, C.; Dore, L. The Millimeter and Submillimeter-Wave Spectrum of Boron Monofluoride: Equilibrium Structure. *J. Mol. Spectrosc.* **1989**, *134*, 159–167 and references therein.
- (12) Endo, Y.; Saito, S.; Hirota, E. Microwave Spectroscopy of Boron Chloride (BCl). The Chlorine Nuclear Quadrupole Coupling Constant. *Bull. Chem. Soc. Jpn.* **1983**, *56*, 3410–3414.
- (13) Nomoto, M.; Okabayashi, T.; Klaus, T.; Tanimoto, M. Microwave spectroscopic study of the BBr molecule. *J. Mol. Struct.* **1997**, *413–414*, 471–476.
- (14) Coxon, J. A.; Naxakis, S. Rotational Analysis of the  $a^3\Pi(0^+, 1) \rightarrow X^1\Sigma^+$  System of <sup>11</sup>BI. *J. Mol. Spectrosc.* **1987**, *121*, 453–464.
- (15) Bettinger, H. F. Phenylborylene: Direct Spectroscopic Characterization in Inert Gas Matrices. *J. Am. Chem. Soc.* **2006**, *128* (8), 2534–2535.
- (16) van der Kerk, S. M.; Boersma, J.; van der Kerk, G. J. M. The Generation and Some Reactions of Methylborylene. *Tetrahedron Lett.* **1976**, *17*, 4765–4766.
- (17) van der Kerk, S. M.; Budzelaar, P. H. M.; van Eekeren, A. L. M.; van der Kerk, G. J. M. The addition of methylborylene to acetylenes. Synthesis of 1,4-diboracyclohexa-2,5-dienes, and of a borirene and a diboretene derivative. *Polyhedron* **1984**, *3*, 271–280.
- (18) Schlögl, R.; Wrackmeyer, B. The System Potassium-Graphite/Methylborondibromide/Alkyne: Query about the Intermediacy of Methylborylene. *Polyhedron* **1985**, *4*, 885–892.
- (19) Claims in refs 16 and 17 (and references therein) that methylborylene was generated as an intermediate, using CH<sub>3</sub>BBr<sub>2</sub> with C<sub>8</sub>K or Na/K alloy, in certain C–H insertion reactions and additions across carbon-carbon multiple bonds were disputed (see

- refs 1, 18, and 20). Schlögl and Wrackmeyer<sup>18</sup> reported an unsuccessful attempt to reproduce syntheses in ref 17.
- (20) Ramsey, B. G.; Bier, M. E. A Laser Desorption Ionization Mass Spectrometry Investigation of Triarylboranes and Tri-9-anthrylborane Photolysis Products. *J. Organomet. Chem.* **2005**, *690*, 962–971.
- (21) Pachaly, B.; West, R. Photochemical Generation of Triphenylsilylboranediyl ( $C_6H_5$ )<sub>3</sub>SiB: from Organosilylboranes. *Angew. Chem., Int. Ed.* **1984**, *23*, 454–455.
- (22) Vidovic, D.; Aldridge, S. Coordination Chemistry of Group 13 Monohalides. *Chem. Sci.* **2011**, *2* (4), 601–608.
- (23) Dull, R. B. Note on the Spectrum of Boron Fluoride. *Phys. Rev.* **1935**, *47*, 458–460.
- (24) Johnson, R. C.; Jenkins, H. G. The Band Spectra of Silicon Fluoride. *Proc. R. Soc. London, Ser. A* **1927**, *116*, 327–351.
- (25) Johnson, R. C.; Tawde, N. R. A Search for the Band Spectra of Boron Fluoride. *Philos. Mag.* **1932**, *13*, 501–504.
- (26) Timms, P. L. Chemistry of Boron and Silicon Subhalides. *Acc. Chem. Res.* **1973**, *6*, 118–123.
- (27) Andrews, L.; Hassanzadeh, P.; Martin, J. M. L.; Taylor, P. R. Pulsed Laser Evaporated Boron Atom Reactions with Acetylene. Infrared Spectra and Quantum Chemical Structure and Frequency Calculations for Several Novel Organoborane  $BC_2H_2$  and  $HBC_2$  Molecules. *J. Phys. Chem.* **1993**, *97*, 5839–5847.
- (28) Braunschweig, H.; Dewhurst, R. D.; Gessner, V. H. Transition Metal Borylene Complexes. *Chem. Soc. Rev.* **2013**, *42*, 3197–3208.
- (29) Soleilhavoup, M.; Bertrand, G. Borylenes: An Emerging Class of Compounds. *Angew. Chem., Int. Ed.* **2017**, *56*, 10282–10292.
- (30) Cowley, A. H.; Lomeli, V.; Voigt, A. Synthesis and Characterization of a Terminal Borylene (Boranediyl) Complex. *J. Am. Chem. Soc.* **1998**, *120*, 6401–6402.
- (31) Maser, L.; Vondung, L.; Langer, R. The ABC in Pincer Chemistry - From Amine- to Borylene- and Carbon-Based Pincer-Ligands. *Polyhedron* **2018**, *143*, 28–42.
- (32) Hadlington, T. J.; Szilvási, T.; Driess, M. Silylene-Nickel Promoted Cleavage of B-O Bonds: From Catechol Borane to the Hydroborylene Ligand. *Angew. Chem. Int. Ed.* **2017**, *56*, 7470–7474.
- (33) Nutz, M.; Borthakur, B.; Prankevicus, C.; Dewhurst, R. D.; Schäfer, M.; Dellermann, T.; Glaab, F.; Thaler, M.; Phukan, A. K.; Braunschweig, H. Release of Isonitrile- and NHC-Stabilized Borylenes from Group VI Terminal Borylene Complexes. *Chem. Eur. J.* **2018**, *24*, 6843–6847.
- (34) Macha, B. B.; Dhara, D.; Radacki, K.; Dewhurst, R. D.; Braunschweig, H. Intermetallic Transfer of Unsymmetrical Borylene Fragments: Isolation of the Second Early-Transition-Metal Terminal Borylene Complex and Other Rare Species. *Dalton Trans.* **2020**, *49*, 17719–17724.
- (35) Bissinger, P.; Braunschweig, H.; Kraft, K.; Kupfer, T. Trapping the Elusive Parent Borylene. *Angew. Chem., Int. Ed.* **2011**, *50*, 4704–4707.
- (36) Kinjo, R.; Donnadiou, B.; Celik, M. A.; Frenking, G.; Bertrand, G. Synthesis and Characterization of a Neutral Tricoordinate Organoboron Isoelectronic with Amines. *Science.* **2011**, *333*, 610–613.
- (37) Wang, H.; Wu, L.; Lin, Z.; Xie, Z. Synthesis, Structure and Reactivity of a Borylene Cation  $[(NHSi)_2B(CO)]^+$  Stabilized by Three Neutral Ligands. *J. Am. Chem. Soc.* **2017**, *139*, 13680–13683.
- (38) Wang, H.; Wu, L.; Lin, Z.; Xie, Z. Transition-Metal-Like Behavior of Monovalent Boron Compounds: Reduction, Migration, and Complete Cleavage of CO at a Boron Center. *Angew. Chem., Int. Ed.* **2018**, *57*, 8708–8713.
- (39) van der Kerk, S. M.; van der Kerk, G. J. M. Insertion of Methylborylene into C-H Bonds. *J. Organomet. Chem.* **1980**, *190*, C11–C13.
- (40) Grigsby, W. J.; Power, P. P. Isolation and Reduction of Sterically Encumbered Arylboron Dihalides: Novel Boranediyl Insertion into C-C  $\sigma$ -Bonds. *J. Am. Chem. Soc.* **1996**, *118*, 7981–7988.
- (41) Braunschweig, H.; Dewhurst, R. D.; Herbst, T.; Radacki, K. Reactivity of a Terminal Chromium Borylene Complex towards Olefins: Insertion of a Borylene into a C-H Bond. *Angew. Chem., Int. Ed.* **2008**, *47*, 5978–5980.
- (42) Donald, K. J.; Befekadu, E.; Prasad, S. Coordination and Insertion: Competitive Channels for Borylene Reactions. *J. Phys. Chem. A* **2017**, *121*, 8982–8994.
- (43) Liu, S.; Légaré, M.-A.; Hofmann, A.; Dellermann, T.; Braunschweig, H. Transition-Metal-Carbene-like Intermolecular Insertion of a Borylene into C-H Bonds. *Chem. Commun.* **2020**, *56*, 7277–7280.
- (44) Edel, K.; Krieg, M.; Grote, D.; Bettinger, H. F. Photoreactions of Phenylborylene with Dinitrogen and Carbon Monoxide. *J. Am. Chem. Soc.* **2017**, *139*, 15151–15159.
- (45) Légaré, M.-A.; Bélanger-Chabot, G.; Dewhurst, R. D.; Welz, E.; Krummenacher, I.; Engels, B.; Braunschweig, H. Nitrogen Fixation and Reduction at Boron. *Science* **2018**, *359*, 896–900.
- (46) Légaré, M. A.; Rang, M.; Bélanger-Chabot, G.; Schweizer, J. I.; Krummenacher, I.; Bertermann, R.; Arrowsmith, M.; Holthausen, M. C.; Braunschweig, H. The Reductive Coupling of Dinitrogen. *Science* **2019**, *363*, 1329–1332.
- (47) Zhang, H.; Yuan, R.; Wu, W.; Mo, Y. Two Push-Pull Channels Enhance the Dinitrogen Activation by Borylene Compounds. *Chem. Eur. J.* **2020**, *26*, 2619–2625.
- (48) Guo, Y.; Yao, Z.; Zhan, S.; Timmer, B. J. J.; Tai, C.-W.; Li, X.; Xie, Z.; Meng, Q.; Fan, L.; Zhang, F.; et al. Molybdenum and Boron Synergistically Boosting Efficient Electrochemical Nitrogen Fixation. *Nano Energy* **2020**, *78*, 105391.
- (49) Wang, Y.; Liu, C.-G. The Use of Main-Group Elements to Mimic Catalytic Behavior of Transition Metals I: Reduction of Dinitrogen to Ammonia Catalyzed by Bis(Lewis Base)Borylenium Diradicals. *Phys. Chem. Chem. Phys.* **2020**, *22* (48), 28423–28433.
- (50) Walawalkar, M. G. Boron: The First *p*-Block Element to Fix Inert  $N_2$  All the Way to  $NH_3$ . *Dalton Trans.* **2021**, *50*, 460–465.
- (51) Kang, B.; Yuan, Y.; Lv, Y.; Ai, H.; Yong Lee, J. Synergistic Ultra-High Activity of Double B Doped Graphyne for Electrocatalytic Nitrogen Reduction. *Chem. Eng. J.* **2022**, *428*, 131318.
- (52) Ito, M.; Tokitoh, N.; Kawashima, T.; Okazaki, R. Formation of a Borylene by Photolysis of an Overcrowded Bis(methylseleno)-borane. *Tetrahedron Lett.* **1999**, *40*, 5557–5560.
- (53) Curran, D. P.; Boussonnière, A.; Geib, S. J.; Lacôte, E. The Parent Borylene: Betwixt and Between. *Angew. Chem., Int. Ed.* **2012**, *51*, 1602–1605.
- (54) Lu, D.; He, Y.; Wu, C. Electronic Structure of Mono(Lewis Base)-Stabilized Borylenes. *Phys. Chem. Chem. Phys.* **2019**, *21*, 23533–23540.
- (55) Bharadwaz, P.; Phukan, A. K. Introducing N-Heterocyclic Borylenes: Theoretical Prediction of Stable, Neutral, Monomeric Boron(I) Carbenoids. *Inorg. Chem.* **2019**, *58*, 5428–5432.
- (56) Donald, K. J.; Gillespie, S.; Shafi, Z. Ouborboros: Heterocycles Closed by Dative  $\sigma$ -Bonds and Stabilized by  $\pi$ -Delocalization. *Tetrahedron* **2019**, *75*, 335–345.
- (57) Báez-Grez, R.; Inostroza, D.; Garcia, V.; Vásquez-Espinal, A.; Donald, K. J.; Tiznado, W. Aromatic Ouborboros: Heterocycles Involving a  $\sigma$ -donor-acceptor Bond and  $4n+2$   $\pi$ -Electrons. *Phys. Chem. Chem. Phys.* **2020**, *22*, 1826–1832.
- (58) Wu, T.; Gray, E.; Chen, B. A Self-Healing, Adaptive and Conductive Polymer Composite Ink for 3D Printing of Gas Sensors. *J. Mater. Chem. C* **2018**, *6* (23), 6200–6207.
- (59) Wu, Q.; Xiong, H.; Zhu, Y.; Ren, X.; Chu, L.-L.; Yao, Y.-F.; Huang, G.; Wu, J. Self-Healing Amorphous Polymers with Room-Temperature Phosphorescence Enabled by Boron-Based Dative Bonds. *ACS Appl. Polym. Mater.* **2020**, *2*, 699–705.
- (60) Matteson, D. S.; Michnick, T. J.; Willett, R. D.; Patterson, C. D. [(1R)-1-Acetamido-3-(Methylthio)Propyl]Boronic Acid and the x-Ray Structure of Its Ethylene Glycol Ester. *Organometallics* **1989**, *8*, 726–729.
- (61) Liu, X.-C.; Hubbard, J. L.; Scouten, W. H. Synthesis and Structural Investigation of Two Potential Boronate Affinity Chromatography Ligands Catechol [2-(Diisopropylamino)

- Carbonyl]Phenylboronate and Catechol [2-(Diethylamino) Carbonyl, 4-Methyl]Phenylboronate. *J. Organomet. Chem.* **1995**, *493*, 91–94.
- (62) Becke, A. D. Density-Functional Thermochemistry. III. The Role of Exact Exchange. *J. Chem. Phys.* **1993**, *98*, 5648–5652.
- (63) Frisch, M. J.; Trucks, G. W.; Schlegel, H. B.; Scuseria, G. E.; Robb, M. A.; Cheeseman, J. R.; Scalmani, G.; Barone, V.; Mennucci, B.; Petersson, G. A.; et al., *Gaussian 09*, Rev. D.01; Gaussian, Inc.: Wallingford, CT, 2013.
- (64) Kendall, R. A.; Dunning, T. H., Jr.; Harrison, R. J. Electron affinities of the first-row atoms revisited. Systematic basis sets and wave functions. *J. Chem. Phys.* **1992**, *96*, 6796–6806.
- (65) Johnson, E. R.; Becke, A. D. A post-Hartree-Fock model of intermolecular interactions: Inclusion of higher-order corrections. *J. Chem. Phys.* **2006**, *124*, 174104.
- (66) Grimme, S.; Ehrlich, S.; Goerigk, L. Effect of the Damping Function in Dispersion Corrected Density Functional Theory. *J. Comput. Chem.* **2011**, *32*, 1456–1465.
- (67) Zhao, Y.; Truhlar, D. G. The M06 Suite of Density Functionals for Main Group Thermochemistry, Thermochemical Kinetics, Noncovalent Interactions, Excited States, and Transition Elements: Two New Functionals and Systematic Testing of Four M06-Class Functionals and 12 Other Functionals. *Theor. Chem. Acc.* **2008**, *120*, 215–241.
- (68) Chai, J.-D.; Head-Gordon, M. Long-Range Corrected Hybrid Density Functionals with Damped Atom-Atom Dispersion Corrections. *Phys. Chem. Chem. Phys.* **2008**, *10*, 6615–6620.
- (69) Frisch, M. J.; Head-Gordon, M.; Pople, J. A. Direct MP2 gradient method. *Chem. Phys. Lett.* **1990**, *166*, 275–280.
- (70) Head-Gordon, M.; Head-Gordon, T. Analytic MP2 Frequencies Without Fifth Order Storage: Theory and Application to Bifurcated Hydrogen Bonds in the Water Hexamer. *Chem. Phys. Lett.* **1994**, *220*, 122–128 and references therein.
- (71) Pople, J. A.; Head Gordon, M.; Raghavachari, K. Quadratic Configuration Interaction. A General Technique for Determining Electron Correlation Energies. *J. Chem. Phys.* **1987**, *87*, 5968–5975 and references therein.
- (72) Schleyer, P. v. R.; Pühlhofer, F. Recommendations for the Evaluation of Aromatic Stabilization Energies. *Org. Lett.* **2002**, *4*, 2873–2876.
- (73) Schleyer, P. v. R.; Maerker, C.; Dransfeld, A.; Jiao, H.; van Eikema Hommes, N. J. R. Nucleus-Independent Chemical Shifts: A Simple and Efficient Aromaticity Probe. *J. Am. Chem. Soc.* **1996**, *118*, 6317–6318.
- (74) Corminboeuf, C.; Heine, T.; Seifert, G.; Schleyer, P.v.R.; Weber, J. Induced Magnetic Fields in Aromatic [n]-Annulenes - Interpretation of NICS Tensor Components. *Phys. Chem. Chem. Phys.* **2004**, *6*, 273–276.
- (75) Dennington, R.; Keith, T. A.; Millam, J. M. *GaussView, Version 6*; Semichem Inc.: Shawnee Mission, KS, 2016.
- (76) *Chemcraft - Graphical software for visualization of quantum chemistry computations*; <https://www.chemcraftprog.com>. Last accessed July 14, 2022.
- (77) Pyykkö, P.; Atsumi, M. Molecular Single-Bond Covalent Radii for Elements 1–118. *Chem. Euro. J.* **2009**, *15*, 186–197.
- (78) Emsley, J. *The Elements*, 3rd ed.; Oxford University, Press: Oxford, U.K.
- (79) The presence of an O–N single bond in the ring (as in systems **4**, **5**, and **8**) appears to guarantee a failure to form stable borylene rings. O–N single bonds are known to be relatively weak (compared to C–O bonds, for example), and it was typically the disruption of that O–N contact and subsequent structural rearrangements that characterized chain formation from the cyclic starting structure for species in classes **4**, **5**, and **8**. Those rearrangements are driven as well by the change from mono- to trivalent boron.
- (80) McKellar, A. R. W.; Bunker, P. R.; Sears, T. J.; Evenson, K. M.; Saykally, R. J.; Langhoff, S. R. Far Infrared Laser Magnetic Resonance of Singlet Methylene: Singlet–Triplet Perturbations, Singlet–Triplet Transitions, and the Singlet–Triplet Splitting. *J. Chem. Phys.* **1983**, *79*, 5251–5264.
- (81) Gibson, S. T.; Greene, J. P.; Berkowitz, J. Photoionization of the Amidogen Radical. *J. Chem. Phys.* **1985**, *83*, 4319–4328.
- (82) Berkowitz, J.; Greene, J. P.; Cho, H.; Rušćić, B. Photoionization Mass-Spectrometric Studies of SiH<sub>n</sub> (n = 1–4). *J. Chem. Phys.* **1987**, *86*, 1235–1248.
- (83) Mukhopadhyay, D. P.; Schleier, D.; Fischer, I.; Loison, J.-C.; Alcaraz, C.; Garcia, G. A. Photoelectron Spectroscopy of Boron-Containing Reactive Intermediates using Synchrotron Radiation: BH<sub>2</sub>, BH, and BF. *Phys. Chem. Chem. Phys.* **2020**, *22*, 1027–1034.
- (84) Gibson, S. T.; Greene, J. P.; Berkowitz, J. Photoionization of the Amidogen Radical. *J. Chem. Phys.* **1985**, *83*, 4319–4328.
- (85) Gordy, W. Dependence of Bond Order and of Bond Energy Upon Bond Length. *J. Chem. Phys.* **1947**, *15*, 305–310.
- (86) Paolini, J. P. The Bond Order - Bond Length Relationship. *J. Comput. Chem.* **1990**, *11*, 1160–1163.
- (87) Fukui, K. The path of chemical-reactions – The IRC approach. *Acc. Chem. Res.* **1981**, *14*, 363–368.
- (88) Hratchian, H. P.; Schlegel, H. B. In *Theory and Applications of Computational Chemistry: The First 40 Years*; Dykstra, C. E., Frenking, G., Kim, K. S., Scuseria, G., Eds.; Elsevier: Amsterdam, 2005; pp 195–249.
- (89) Arduengo, A. J., III; Dias, H. V. R.; Harlow, R. L.; Kline, M. Electronic Stabilization of Nucleophilic Carbenes. *J. Am. Chem. Soc.* **1992**, *114*, 5530–5534.

## Recommended by ACS

### C–C versus C–H Activation: Understanding How the Carbene $\pi$ -Accepting Ability Controls the Intramolecular Reactivities of Mono(carbene)-Stabil...

Linlin Wu, Zhenyang Lin, et al.

MARCH 08, 2021  
ORGANOMETALLICS

READ 

### Understanding the Diverse Reactivity of Pentaphenylborole toward Epoxides

Xueying Guo, Zhenyang Lin, et al.

OCTOBER 21, 2020  
THE JOURNAL OF ORGANIC CHEMISTRY

READ 

### [1,5]-Sigmatropic Shifts Regulated by Built-in Frustration

Dinesh V. Vidhani, Igor V. Alabugin, et al.

JUNE 29, 2020  
THE JOURNAL OF PHYSICAL CHEMISTRY A

READ 

### Dissecting Transmetalation Reactions at the Molecular Level: Phenyl Transfer in Metal Borate Complexes

Thomas Auth, Richard A. J. O'Hair, et al.

NOVEMBER 14, 2019  
ORGANOMETALLICS

READ 

Get More Suggestions >